J. A. Mehne. The author is greatly indebted to C. Erginsoy and G. H. Vineyard for their provision of GRAPE program decks and to R. A. Johnson for his provision of "Johnson's Program" decks. Technical discussions with J. W. Corbett, C. Erginsoy, R. A. Johnson, B. Ralph, W. F. Schilling, G. H. Vineyard, and T. O. Ziebold were particularly rewarding.

APPENDIX

An interatomic potential for tungsten was constructed which had the same form as does Potential III of Erginsoy *et al.*[7] for α-iron. It consisted of an exponentially screened Coulomb potential for $r \leq 1$ Å joined to a simple exponential for $r > 1$ Å

$$\phi(r) = (24500/r)\exp(-4.55r), \quad r \leq 1 \text{ Å};$$
$$\phi(r) = 24500\exp(-4.55r), \quad r > 1 \text{ Å}.$$

This potential is compared with the Bohr, Girifalco-Weizer,[43] Johnson,[10] and Thomas-Fermi potentials in Fig. 21. At small separations distances ($r < 0.4$ Å)$\phi(r)$ fits the Thomas-Fermi potential for tungsten. It is equal to the Morse potential of Girifalco and Weizer at $r = 1$ Å and to Johnson's potential at 2.2 Å.

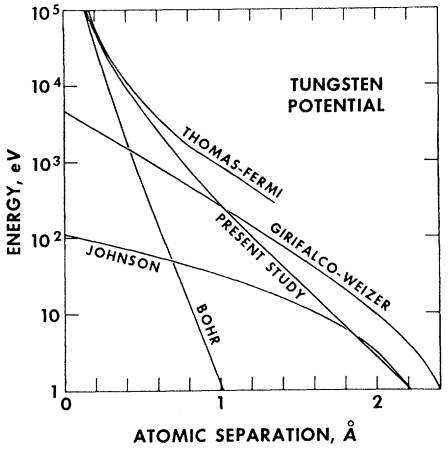

FIG. 21. Tungsten potential used in the present study compared with two high-energy and two low-energy potentials for tungsten.

[43] L. A. Girifalco and V. G. Weizer, Phys. Rev. **114**, 687 (1959).

PHYSICAL REVIEW VOLUME 150, NUMBER 2 14 OCTOBER 1966

Crystal Dynamics of Potassium. I. Pseudopotential Analysis of Phonon Dispersion Curves at 9°K

R. A. COWLEY, A. D. B. WOODS, AND G. DOLLING
Chalk River Nuclear Laboratories, Chalk River, Ontario, Canada
(Received 23 May 1966)

The frequencies of normal modes of vibration of potassium at 9°K have been measured by inelastic-neutron-scattering techniques. Certain selected frequencies are (units 10^{12} cps): H_{15} 2.21±0.02, P_4 1.78$_5$ ±0.02, N_1' 2.40±0.04, N_3' 1.50±0.02$_5$, and N_4' 0.53±0.02. The results are very similar, apart from a scale factor 1.65, to those for sodium. Analysis of the results has been carried out in terms both of conventional Born–von Kármán models and of potential functions defined in reciprocal space. A fifth-neighbor, axially symmetric force model has been used to compute the frequency distribution function for the normal modes and the associated heat capacity. The reciprocal-space analysis was performed in two ways: (a) in terms of a total potential function, whose Fourier transform is the effective interatomic potential between "neutral pseudo-atoms" of potassium, and (b) in terms of the screened pseudopotential for the conduction-electron–ion interaction. Analysis (a) shows that a wide variety of interatomic potentials, both with and without long-range oscillatory character, can be found which give a satisfactory fit to the results. These potentials are compared with those obtained from an analysis of x-ray scattering data for liquid potassium. The pseudopotentials obtained from analysis (b) are in good agreement with that derived by Bortolani from the Heine-Abarenkov model. A reanalysis of the phonon dispersion curves for sodium leads to very similar conclusions, confirming earlier work by Cochran.

1. INTRODUCTION

THE crystal dynamics of metals has received considerable experimental and theoretical attention over the past decade. A large amount of experimental information on dispersion relations $\nu(\mathbf{q})$ of frequency ν versus wave vector $\mathbf{q}$ exists for a number of metals, while theoretical attention has been concentrated principally on the alkali metals.[1] Measurements of $\nu(\mathbf{q})$ for sodium[2] showed that while quite long-range effective forces were present, they were not very strong, and no

[1] For a general review of phonon dispersion curves in metals see G. Dolling and A. D. B. Woods, in *Thermal Neutron Scattering*, edited by P. A. Egelstaff (Academic Press Inc., New York, 1965), Chap. V.

[2] A. D. B. Woods, B. N. Brockhouse, R. H. March, A. T. Stewart, and R. Bowers, Phys. Rev. **128**, 1112 (1962).

definite Kohn anomalies,[3] such as had been observed in lead,[4] and other metals,[1] were present. Analysis of the dispersion curves in terms of a pseudopotential was carried out by Cochran[5,6] and resulted in an effective interatomic potential. At large distances this potential has an oscillatory character, and Koenig[7] showed that this could arise from the discontinuity in the slope of the dielectric screening function, i.e., another aspect of the Kohn effect. Cochran[6] suggested, however, that the oscillations might result from his method of calculating the effective potential.

Attempts to improve the accuracy of the sodium $\nu(\mathbf{q})$ and to measure neutron-scattering line shapes as a function of temperature[8,9] were made difficult by the large incoherent neutron-scattering cross section for sodium. In addition, the occurrence of the martensitic transformation in sodium made it necessary to carry out the experiments above 40°K, where it is possible that line shapes and frequencies are already affected by anharmonic interactions. Because it was felt to be desirable to have a large body of precise information about all aspects of the lattice dynamics of an alkali metal, it was decided to pursue the measurements on a more favorable material; potassium was chosen for several reasons: (1) The ratio of coherent to incoherent scattering cross sections is about two and a half times larger than for sodium. (2) Its electronic properties are nearly ideally free-electron-like, in common with sodium but in contrast with many other metals. (3) No martensitic transformation exists; thus experiments can be done at low temperatures. (4) Large single crystals were available.[10]

Accordingly, the dispersion curves have been measured at a temperature of 9°K and the results interpreted on the basis of a pseudopotential similar to that derived for sodium. The results have also been fitted to a Born–von Kármán model which was then used to calculate the density of phonon states, $g(\nu)$, and hence thermodynamic properties such as the heat capacity. A large part of this paper describes the methods used in this analysis, and the results of several different approaches to calculating an effective interatomic potential as well as the pseudopotential for electron-phonon scattering. It is hoped that these results will assist in the understanding of electron-phonon interaction in metals. It is further intended that these experimental measurements and theoretical calculations will serve as the basis for more extensive studies of the effect of temperature on the phonon spectrum.

2. EXPERIMENT

The phonon dispersion curves have been measured along the high symmetry lines Δ, Σ, $\Lambda(F)$, D, and G (in previous notation[1] $[00\zeta]$, $[\zeta\zeta 0]$, $[\zeta\zeta\zeta]$, $[\frac{1}{2}\frac{1}{2}\zeta]$, and

TABLE I. Normal-mode frequencies (units 10^{12} cps) in potassium at 9°K. The reduced wave-vector coordinates ζ are expressed in units of $(a/2\pi)$, where a is the lattice constant.

ζ	ν $[00\zeta]\Delta_1$	ν $[00\zeta]\Delta_5$	ν $[\zeta\zeta\zeta]\Lambda_3, F_3$
0.15	0.66 ±0.04	0.52±0.03	···
0.20	0.89 ±0.02$_5$	0.68±0.02$_5$	0.77 ±0.05
0.25	1.08 ±0.05	0.82±0.03	1.00 ±0.06
0.30	1.21 ±0.03	0.99±0.02	1.20 ±0.06
0.35	1.35 ±0.04	1.15±0.03	···
0.40	1.53 ±0.03	1.28±0.02$_5$	1.53 ±0.05
0.45	1.63 ±0.03	1.44±0.03	1.68 ±0.04
0.50	1.74 ±0.03$_5$	1.57±0.02	1.78$_5$±0.02
0.55	1.81 ±0.04	1.69±0.02	1.91 ±0.04
0.60	1.89 ±0.03	1.79±0.02$_5$	2.00 ±0.04
0.65	1.96 ±0.06	1.89±0.02	2.05 ±0.06
0.70	1.96$_5$±0.04	1.99±0.02	2.09 ±0.03
0.75	2.08$_5$±0.03	2.07±0.03	2.12 ±0.04
0.80	2.11 ±0.02$_5$	2.11±0.02$_5$	2.16 ±0.03
0.85	2.15 ±0.03	2.19±0.04	2.19 ±0.03
0.90	2.19 ±0.02$_5$	2.20±0.03	2.18 ±0.02$_5$
0.95	2.21 ±0.02$_5$	2.21±0.04	2.22 ±0.03
1.00	2.21 ±0.02	···	···
	$[\frac{1}{2}\frac{1}{2}\zeta]D_1$	$[\frac{1}{2}\frac{1}{2}\zeta]D_3$	$[\frac{1}{2}\frac{1}{2}\zeta]D_4$
0.10	1.52 ±0.04	2.35±0.06	0.70 ±0.03
0.20	1.62 ±0.04	2.30±0.03$_5$	0.97 ±0.03
0.30	1.69 ±0.04	2.20±0.05	1.27 ±0.03
0.40	1.72 ±0.04	2.01±0.04	1.55 ±0.04
	$[\zeta\zeta 0]\Sigma_1$	$[\zeta\zeta 0]\Sigma_3$	$[\zeta\zeta\zeta]\Lambda_1$
0.05	···	···	0.53 ±0.03
0.10	0.74 ±0.02	···	0.95 ±0.02
0.15	1.08 ±0.03	0.67±0.03	1.34 ±0.04
0.20	1.41 ±0.02	0.93±0.03	1.69$_5$±0.02
0.25	1.69 ±0.05	1.11±0.03	1.95 ±0.04
0.30	1.94 ±0.03	1.23±0.03	2.10 ±0.02$_5$
0.35	2.08 ±0.05	1.36±0.03	2.19 ±0.05
0.40	2.25 ±0.03$_5$	1.44±0.02$_5$	2.15 ±0.02$_5$
0.45	2.33 ±0.06	1.49±0.05	2.03 ±0.06
0.50	2.40 ±0.04	1.50±0.02$_5$	···

ζ	ν $[\zeta\zeta 1]G_1$	ν $[\zeta\zeta 1]G_3$	ζ	ν $[\zeta\zeta\zeta]F_1$[a]
0.05	2.22±0.05	2.18 ±0.05	0.55	1.55 ±0.04
0.10	2.14±0.04	2.13 ±0.04	0.58	1.38 ±0.05
0.15	2.01±0.06	2.10 ±0.03$_5$	0.60	1.24 ±0.03
0.20	1.78±0.03	2.02 ±0.03$_5$	0.62	1.17 ±0.03
0.25	1.55±0.04	1.89$_5$±0.03	0.65	1.04 ±0.02$_5$
0.30	1.31±0.04	1.78 ±0.02$_5$	0.68	1.00$_5$±0.02$_5$
0.35	1.07±0.04	1.70 ±0.04	0.70	1.02 ±0.03
0.40	0.81±0.03	1.57 ±0.03	0.72	1.06 ±0.03
0.45	0.61±0.03	1.53 ±0.04	0.75	1.20 ±0.03
0.50	0.53±0.02	···	0.78	1.36 ±0.03
			0.80	1.47 ±0.02
			0.85	1.77 ±0.03
			0.90	1.99 ±0.03
			0.95	2.19 ±0.04

[a] Continuation of Λ branch.

[3] W. Kohn, Phys. Rev. Letters **2**, 393 (1959).
[4] B. N. Brockhouse, T. Arase, G. Caglioti, K. R. Rao, and A. D. B. Woods, Phys. Rev. **128**, 1099 (1962).
[5] W. Cochran, Proc. Roy. Soc. (London) **A276**, 308 (1963).
[6] W. Cochran, in *Inelastic Scattering of Neutrons in Solids and Liquids* (International Atomic Energy Agency, Vienna, 1965), Vol. I, p. 3.
[7] S. H. Koenig, Phys. Rev. **135**, A1693 (1964).
[8] A. D. B. Woods, B. N. Brockhouse, R. H. March, and R. Bowers, Bull. Am. Phys. Soc. **6**, 261 (1961).
[9] See B. N. Brockhouse, A. D. B. Woods, G. Dolling, and I. M. Thorson, in *Proceedings of the Third United Nations International Conference on the Peaceful Uses of Atomic Energy* (United Nations, New York, 1965), Vol. 7, Paper P/12, p. 419.
[10] We are extremely grateful to P. A. Penz for growing two excellent specimens for the purpose of these experiments.

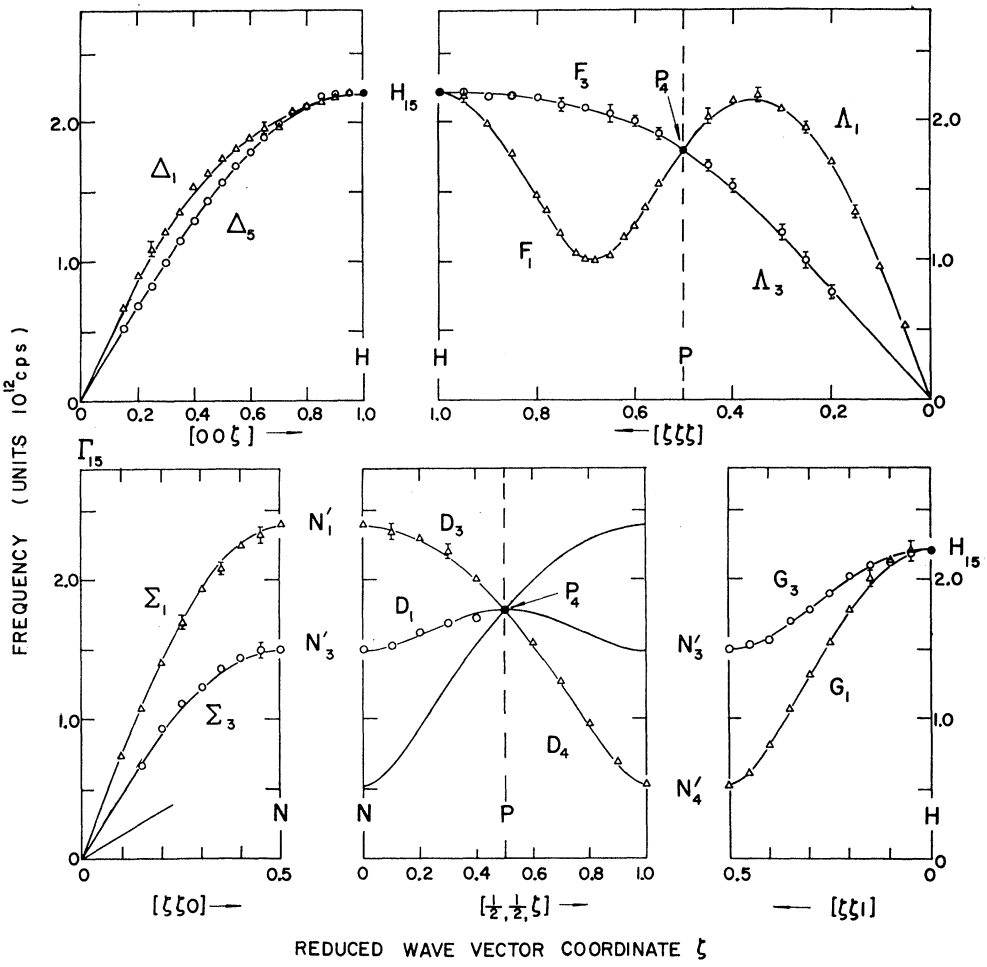

FIG. 1. Measured dispersion curves for potassium at 9°K. $\zeta(2\pi/a)$ is a reduced wave-vector coordinate. In the [00ζ], [ζζ0], and [ζζζ] directions, transverse (longitudinal) modes of vibration are denoted by circles (triangles). The solid curves represent the best fit to the results on the basis of a Born–von Kármán model with axially symmetric forces extending to fifth-nearest-neighbor atoms.

[ζζ1], respectively) at 9°K, using the Chalk River triple-axis crystal spectrometer in its constant-momentum-transfer (constant **Q**) mode of operation.[11] All of the measurements were carried out by observation of neutron-energy-loss processes with variable incident energy; the (aluminum) analyzer was set to observe several neutron energies in the region of 0.012 eV.

The results are shown in Fig. 1 and Table I. The fitted curves shown in Fig. 1 will be discussed in Sec. 3. Inspection reveals that, apart from a scale factor of approximately 1.65, they are very similar in shape to the corresponding curves for sodium[2]—a not unexpected result. The same kind of correspondence, though not quite so close, exists between these results and those for the alloy β-brass (CuZn).[12]

In common with the sodium dispersion curves the Δ_1 and Δ_5 branches appear to cross near $\zeta=0.75$. It is difficult to confirm this point, however, and we are hesitant about drawing any conclusions about the shapes of the curves in this region; they are very close together, and the possibility of double-scattering processes[13] introduces an uncertainty in the identification of observed peaks with particular modes. With the possible exception of these branches near $\zeta=0.75$, the curves are quite smooth and show no evidence of any Kohn anomalies.

3. ANALYSIS OF RESULTS

The measured normal-mode frequencies have been analyzed in two ways: (a) using the method of Born and von Kármán[14] to obtain interatomic force constants (in real space) between near-neighbor atoms, and (b) in terms of potentials defined in reciprocal space, in a similar manner to that employed by Cochran[5] for sodium.

A. Born–von Kármán Analysis

The processes of setting up equations of motion for the atoms in a monatomic bcc crystal, and of the re-

[11] B. N. Brockhouse, in *Inelastic Scattering of Neutrons in Solids and Liquids* (International Atomic Energy Agency, Vienna, 1961), p. 113.

[12] G. Gilat and G. Dolling, Phys. Rev. 138, A1053 (1965).

[13] Reference 1, p. 196, and Ref. 4.

[14] M. Born and K. Huang, *Dynamical Theory of Crystal Lattices* (Clarendon Press, Oxford, England, 1954).

TABLE II. Force constants (units dyn/cm) of model A (up to 5th nearest-neighbor axially symmetric forces). The notation for the Born–von Kármán constants α_i, β_i is that of Ref. 2.

Neighbor(i)	Radial	Tangential	α_i	β_i
1	2576	−109	786	895
2	432	29	432	29
3	−95	12	−41	12
4	3	−4	2	−4
5	15	2	6	4

duction of these equations to a (3×3) dynamical matrix whose eigenvalues are proportional to the squares of the normal-mode frequencies, are too well known to require discussion here.[1] The measured dispersion curves have been fitted by the method of (linear) least squares to a variety of force models involving axially symmetric (A-S)[15] forces extending as far as 10th-nearest-neighbor atoms. The employment of general tensor, rather than A-S forces, produced no significant improvement in the fits to the data. A satisfactory fit was achieved with a 6-parameter A-S model involving forces extending to 3rd-nearest neighbors. Inclusion of more distant neighbor force constants produced only small improvements in the quality of fit. The effect of fitting models to the present measurements in conjunction with the measured elastic constants[16] was also investigated. Values of the elastic constants may be derived from the initial slopes of the dispersion curves at small wave vectors. These values differ significantly (8% for C_{11}, for example) from those obtained from ultrasonic measurements. Nevertheless, a fully satisfactory fit to all the data was achieved with an A-S model (model A) involving forces

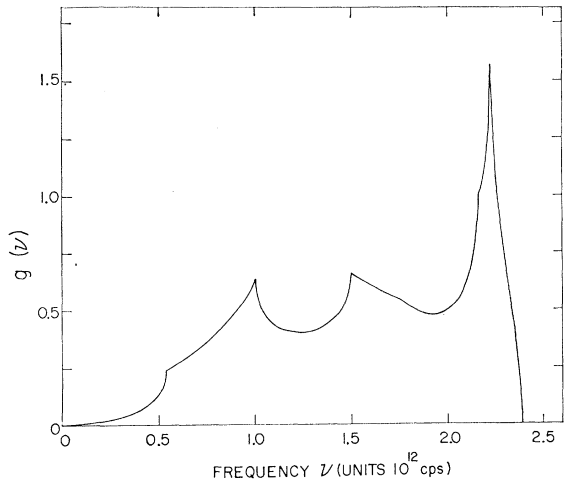

FIG. 2. The frequency distribution function $g(\nu)$ for the normal modes in potassium at 9°K, calculated from the model shown in Fig. 1. A sample of 60 466 176 normal modes was employed to produce this histogram.

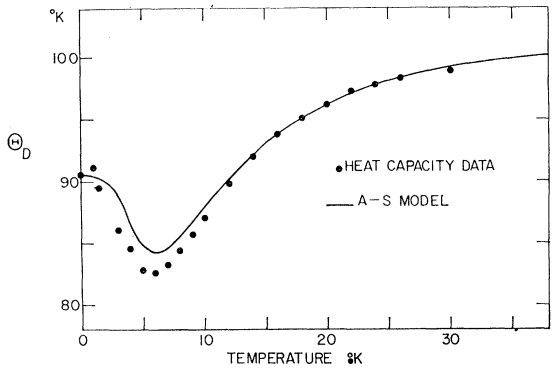

FIG. 3. Equivalent Debye temperatures for potassium, computed in the harmonic approximation from the distribution of Fig. 2, and compared with experimental heat-capacity data (Ref. 18).

extending to 5th-nearest-neighbor atoms. The best-fit values for the 10 force constants of this model (one "radial" and one "tangential" constant for each type of neighbor) are given in Table II, together with the Born–von Kármán constants derived from them. The relationships between these various constants are conveniently listed in Ref. 5. The quality of the fit to the data is illustrated by the curves in Fig. 1. The frequency distribution function $g(\nu)$ for the normal modes has been computed by means of the extrapolation method[17] from the parameters of model A. The result of sampling 60 466 176 normal-mode frequencies from the first Brillouin zone is shown in Fig. 2. From this function it is straightforward to calculate the variation of the heat capacity with temperature, in the harmonic approximation. In view of the very low temperature for which the model is appropriate, one might expect to obtain good agreement with the heat capacity observed at low temperatures, and such is indeed the case. The equivalent Debye temperatures obtained from the calculated and observed heat capacity,[18] as shown in Fig. 3, agree to better than 2% over the range 0 to 30°K, though there appears to be a systematic discrepancy (about 1.8%) near the minimum of the curve between 2 and 8°K. We may also compare theoretical and experimental values[18] of the moments of $g(\nu)$, or the equivalent "Debye frequencies" ν_n derived[19] from these moments. The agreement is good for $n \leq 2$ (see the dashed curve of Fig. 4) and only ν_6 shows a discrepancy larger than experimental error. Figure 4 also shows the effect of using a force model fitted only to the neutron-scattering data, omitting the elastic constants. The poor agreement for $n \leq -2$ arises from the above-mentioned inconsistencies between initial slopes and elastic constants. This does not necessarily imply that either type of measurement is in error, since the ultrasonic

[15] T. Wolfram, G. W. Lehman, and R. E. DeWames, Phys. Rev. **129**, 2483 (1963).
[16] W. R. Marquardt and J. Trivisonno, J. Phys. Chem. Solids **26**, 273 (1965).
[17] G. Gilat and G. Dolling, Phys. Letters **8**, 304 (1964).
[18] D. L. Martin, Phys. Rev. **139**, A150 (1965), and references cited therein.
[19] T. H. K. Barron, W. T. Berg, and J. A. Morrison, Proc. Roy. Soc. (London) **A242**, 478 (1957).

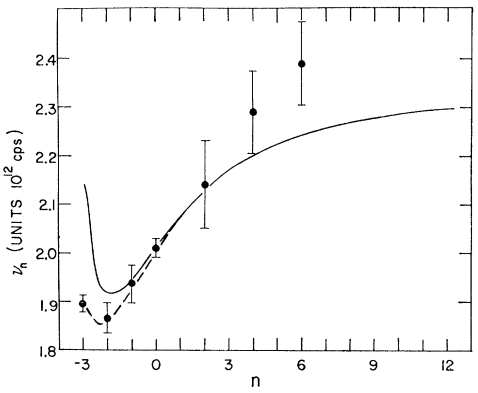

FIG. 4. Equivalent Debye frequencies derived from the moments of the distribution of Fig. 2, dashed curve, compared with experimental heat-capacity data (Ref. 18). The solid curve shows the effect of utilizing a force model fitted only to the results in Fig. 1, ignoring the measured elastic constants.

measurements refer to vibration frequencies $\leq 10^9$ cps, far below the lowest value (5×10^{11} cps) obtained in the neutron-scattering experiments. At 5°K, the heat capacity is dominated by modes of intermediate frequencies ($\lesssim 10^{11}$ cps).

B. Reciprocal-Space Analysis

The normal-mode frequencies ν are given by the equation[14]

$$4\pi^2 m\nu^2 U_\alpha(\mathbf{q})=\sum_\beta D_{\alpha\beta}(\mathbf{q})U_\beta(\mathbf{q}), \tag{1}$$

where

$$D_{\alpha\beta}(\mathbf{q})=\sum_l \phi_{\alpha\beta}(0,l)\exp(i\mathbf{q}\cdot\mathbf{r}_l); \tag{2}$$

$U_\alpha(\mathbf{q})$ specifies the polarization of the mode, $\phi_{\alpha\beta}(0,l)$ represents force constant linking the atom at an origin (0) with that at position $\mathbf{r}_l$. We assume an axially symmetric two-body interaction $V(r)$ between the atoms, dependent only on the distance between them:

$$\phi_{\alpha\beta}(0,l)=\left[\frac{d^2V(r)}{du_\alpha(0)du_\beta(l)}\right]_{r=r_l}, \quad l\neq 0,$$
$$\phi_{\alpha\beta}(0,0)=-\sum\phi_{\alpha\beta}(0,l), \qquad l\neq 0 \tag{3}$$

where $u_\alpha(l)$ is the displacement from equilibrium of the atom l. We now express $V(r)$ in terms of its Fourier transform

$$V(r)=(2\pi)^{-3}v\int V(Q)\exp(-i\mathbf{Q}\cdot\mathbf{r})d\mathbf{Q}, \tag{4}$$

where v is the volume of the unit cell and $V(Q)$ depends only on $|\mathbf{Q}|$. Substituting Eqs. (3) and (4) into (2), and taking into account the term $\phi_{\alpha\beta}(0,0)$ we obtain[20]

$$D_{\alpha\beta}(\mathbf{q})=\sum_\tau[(q_\alpha+\tau_\alpha)(q_\beta+\tau_\beta)V(\mathbf{q}+\boldsymbol{\tau})-\tau_\alpha\tau_\beta V(\boldsymbol{\tau})], \tag{5}$$

where $\boldsymbol{\tau}=(\tau_\alpha,\tau_\beta,\tau_\gamma)$ represents a vector of the reciprocal lattice of the crystal, and $\mathbf{q}+\boldsymbol{\tau}=\mathbf{Q}$. Following Cochran we may subdivide this expression for the dynamical matrix element into three contributions

$$D_{\alpha\beta}(q)=D^R+D^C+D^E. \tag{6}$$

These terms represent contributions arising from short-range overlap forces, long-range electrostatic forces between the bare ions, and interactions involving the conduction electrons and the ions, respectively. Recent work by Vosko[21] has strongly suggested that D^R is very small indeed for both Na and K, and in most of our calculations we have neglected this contribution. (Introduction of a small overlap force produces no significant change in any of the results discussed below.) The "Coulomb" contribution D^C is easily calculated with the help of the Ewald θ transformation, leaving only the conduction-electron term D^E to be dealt with. Two different methods of analysis suggest themselves:

(a) To subtract from the observed phonon frequencies [i.e., the $D_{\alpha\beta}(\mathbf{q})$] the known contribution D^C, as was done by Cochran for sodium,[5] and to fit the remainder to some function $V^E(\mathbf{Q})$ corresponding to the contribution D^E. A refinement of this procedure is to assume a local pseudopotential model for the conduction electron-ion interaction: If $V_p(Q)$ is the Fourier transform of the local pseudopotential (we omit the vector sign to emphasize the axial symmetry of the potentials), and $\epsilon(Q)$ is the dielectric function, we have

$$V^E(Q)=(v/4\pi e^2)Q^2(1-\epsilon^{-1}(Q))|V_p(Q)|^2. \tag{7}$$

The experimental results are then fitted to the screened potential $V_p(Q)/\epsilon(Q)$. The advantage of this is that, as shown by recent calculations of Animalu[22] and by Bortolani,[23] $V_p(Q)/\epsilon(Q)$ is of oscillating sign. Thus, while $V^E(Q)$ is always non-negative, it displays cusp-like singularities at Q values for which $V_p(Q)=0$. It is therefore much easier and more satisfactory to fit the experimental data with the fairly well-behaved screened potential than with $V^E(Q)$ itself.

(b) To analyze the total $D_{\alpha\beta}(\mathbf{q})$ in terms of a potential function $V^T(\mathbf{Q})$, using Eq. (5). This total potential is the Fourier transform of the effective ion-ion potential in real space, whose first and second derivatives at the interatomic distances give the conventional Born–von Kármán force constants. We might refer to this as the potential between "neutral pseudo-atoms".[24]

Both methods of analysis have been carried out in the same manner, as follows: It is convenient to define new functions $G^E(Q)$ and $G^T(Q)$:

$$V^E(Q)=\frac{e^2}{Q^2v}G^E(Q); \quad V^T(Q)=\frac{e^2}{Q^2v}G^T(Q). \tag{8}$$

In the first instance the functions $G^E(Q)$ and $G^T(Q)$

[20] D. Pines, *Elementary Excitations in Solids* (W. A. Benjamin, Inc., New York, 1963), p. 26.

[21] S. H. Vosko, Phys. Letters **13**, 97 (1964).

[22] A. O. E. Animalu, Technical Report No. 3, Solid State Theory Group, Cavendish Laboratory, Cambridge, 1965 (unpublished).

[23] V. Bortolani (private communication).

[24] J. M. Ziman, Advan. Phys. **13**, 89 (1964).

were specified by a Fourier series of up to 30 terms:

$$G(Q)=A_0-[1-\cos(\pi Q/Q_{\max})](2\pi+\sum_{n\ \text{odd}} A_n)$$
$$+\sum_{n=1}^{n_{\max}} A_n[1-\cos(n\pi Q/Q_{\max})],$$

where $Q_{\max}$ is some upper limit beyond which the two functions $G(Q)$ are assumed to be negligible. A_0 is a constant, equal to 4π for $G^E(Q)$ and zero for $G^T(Q)$. The form of the first part of this expression was chosen so that the $G(Q)$ would tend smoothly to their respective limits at $Q=0$ and $Q_{\max}$. The coefficients A_n were then obtained by the method of linear least-squares fitting to either $D_{\alpha\beta}(=D^C+D^E)$ or D^E, as the case may be. This procedure, although most efficient, was found to be unsatisfactory owing to the existence of "ripples" in the fitted G functions arising from the large n terms in the Fourier series. These fitted G functions could, however, be used as the first stage of a nonlinear least-squares fitting procedure in which the function is specified by a table of values at between 10 and 30 selected Q values. Values of G at intermediate $Q=Q_i$ are found by Lagrange (cubic) interpolation, using the two nearest tabulated values on either side of Q_i. The same method was used in the process of fitting D^E by means of a tabulated $V_p(Q)/\epsilon(Q)$ function. By definition, $G^E(0)=4\pi$ and $G^T(0)=0$, and the screened pseudopotential $V_p(Q)/\epsilon(Q)$ tends to a finite value at $Q=0$. We assume a value $Q=Q_{\max}$, beyond which $G^E(Q)=G^T(Q)=V_p(Q)/\epsilon(Q)=0$. The fitting process is initiated by specifying a table of values for the function concerned at Q values between 0 and $Q_{\max}$, and imposing the condition that the function tend smoothly to zero at $Q_{\max}$. These tabular values constitute the variable parameters of the least-squares fit. The phonon frequencies for any given reduced wave vector $\mathbf{q}$ may now be computed from Eqs. (1) and (5) through (8). The computation is simplified if $\mathbf{q}$ lies along a direction of high symmetry, since the dynamical matrix factorizes into three equations involving linear combinations of the $D_{\alpha\beta}(\mathbf{q})$. The number of lattice points $\boldsymbol{\tau}$ involved in the summation of Eq. (5) becomes very large as $Q_{\max}$ increases, as does the number of tabular values required for adequate specification of the function. These factors effectively restrict the choice of $(a/2\pi)Q_{\max}$ to less than about 2.8; indeed, there seem to be insufficient data at present to specify the G functions much beyond 2.4. (For comparison, the calculations previously carried out[5] for Na assumed a cutoff at $aQ/2\pi=\sqrt{2}$.) Calculation of phonon frequencies from the screened pseudopotential involves a knowledge of the dielectric function $\epsilon(Q)$. We have employed both the expression given by Bardeen[25] and also that proposed by Heine and Abarenkov,[26] which incorporates certain corrections (e.g., for exchange effects) to the simple Bardeen formula.

[25] J. Bardeen, Phys. Rev. **52**, 689 (1937).
[26] V. Heine and I. Abarenkov, Phil. Mag. **9**, 451 (1964).

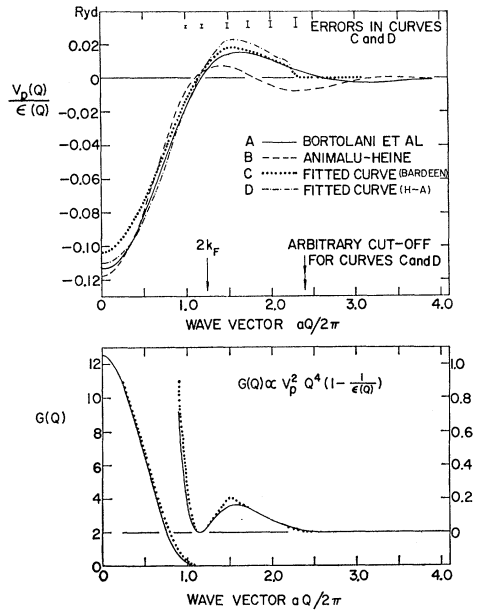

FIG. 5. The screened pseudopotential $V_p(Q)/\epsilon(Q)$ for the conduction electron-ion interaction in potassium at 9°K (upper diagram). A and B are theoretical curves based on the Heine-Abarenkov model, while C and D are fitted to the results of Fig. 1, as described in the text. The lower diagram shows the function $G^E(Q)$ derived from curves A (solid) and C (dotted) above. The large wave-vector region is shown on a 10× scale on the right.

The results of these least-squares fitting calculations for potassium, with $(a/2\pi)Q_{\max}$ chosen to be 2.4, are shown in Fig. 5 (upper diagram) both for the Bardeen (curve C) and Heine-Abarenkov (curve D) dielectric functions. Two screened pseudopotentials calculated on the basis of the Heine-Abarenkov model[22,23] are also shown in curves A and B, respectively. The downward kink in the curves C and D near $Q_{\max}$ results from the condition that V_p/ϵ goes smoothly to zero at $Q_{\max}$. As $Q_{\max}$ is changed, the quality of the fit to the phonon frequencies increases as $Q_{\max}$ increases, but the same general shape of curve results. If $(a/2\pi)Q_{\max}$ is increased beyond 2.4, then the calculated errors of the tabulated values of the curve increases, showing that there are insufficient data to determine them.

The phonon frequencies calculated from curves C and D are an excellent fit to the measurements, similar to that shown in Fig. 1. As would be expected from the close similarity of our curve, D, with that of Bortolani,[23] A, and the contrast with that of Animalu,[22] B, the fit to experiment given by use of A is substantially better than that obtained with B. The lower part of Fig. 5 shows the function $G^E(Q)$ derived from curves A and C above. Note the enlarged scale for $aQ/2\pi>1$ to show the details more clearly.

In Fig. 6 we show the results of calculations of the function $G^T(Q)$ for various $Q_{\max}$. All these curves provide a satisfactory fit to the experimental data, but the increase in size of error bars as $Q_{\max}$ increases is much more pronounced than in the screened-pseudopotential

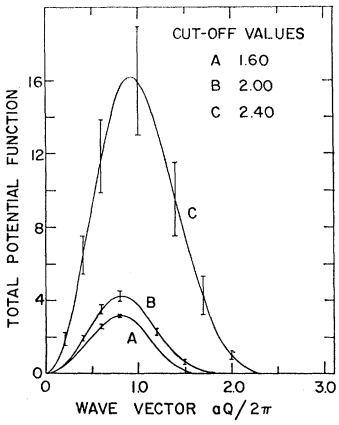

FIG. 6. The total potential function $G^T(Q)$ derived from the results of Fig. 1, for various values of the cutoff wave vector Q_{max} for potassium at 9°K. Typical error bars are indicated at arbitrary intervals. For $(a/2\pi)Q_{max} \geq 2.4$, the error bars become very large, indicating insufficient data to specify the function.

calculations. As mentioned earlier, the Fourier transforms of these curves and their derivatives represent effective potentials (and derivatives thereof) in real space between the potassium atoms, including conduction-electron effects. The existence of many different functions $G^T(Q)$, all of which fit the experimental data, merely reflects the fact that the interatomic potential $V(r)$ for all r cannot be determined from a knowledge of phonon frequencies alone. Nevertheless, it seems of interest to compute $V(r)$ for the various $G^T(Q)$. The results for $Q_{max}(a/2\pi)=1.6$ (curve A of Fig. 6) are shown in Fig. 7. The values of $(1/r)\,dV/dr$ and d^2V/dr^2 at the atomic positions are simply related to the force constants of a conventional Born–von Kármán analysis. The derivatives shown in Fig. 7 are in good agreement with the force constants obtained in the Born–von Kármán analysis of Sec. 3 A. After the initial oscillation at the near-neighbor distance, $V(r)$ falls smoothly and monotonically to zero, in marked contrast to the interatomic potential deduced[27] for liquid potassium from x-ray scattering data. Transformation of curve C of Fig. 6, however, leads to a long-range oscillatory potential $V(r)$, similar in character to the dashed curve in Fig. 7. Thus, in the case of solid potassium, it is possible to construct long-range oscillatory potentials which are consistent with the measured phonon frequencies. However, such potentials are certainly not necessary and seem less physically plausible than the potential shown as a solid line in Fig. 7.

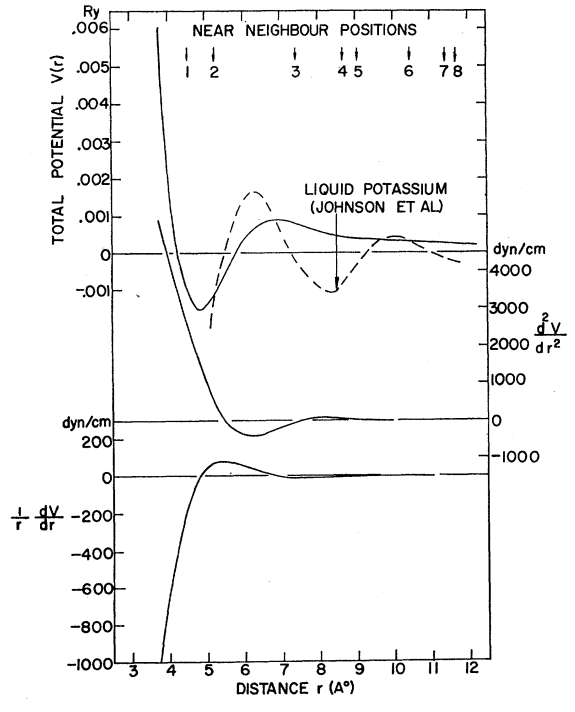

FIG. 7. The effective interatomic potential and its derivatives for potassium at 9°K, obtained by Fourier transformation of curve A, Fig. 6. The dashed curve is one of several similar oscillatory potentials derived (Ref. 27) from x-ray scattering data for liquid potassium.

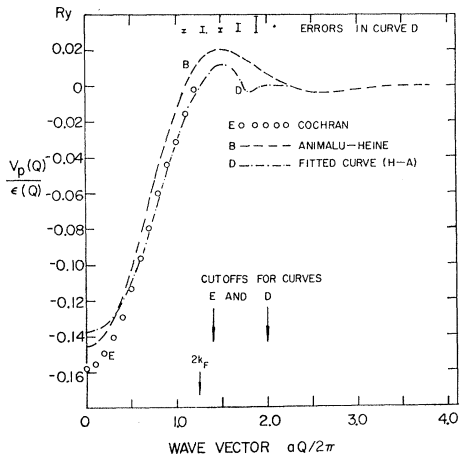

FIG. 8. The screened pseudopotential $V_p(Q)/\epsilon(Q)$ for the conduction electron-ion interaction in sodium. The labels B and D are the same as for Fig. 5. Curve E (open circles) is that derived by Cochran (Ref. 5) from the function $G^E(Q)$.

We have also performed the above analysis for the case of sodium, using the normal-mode frequencies obtained by Woods *et al.*[2] As in the case of potassium, we again assumed the short-range interaction D^R to be negligible. The results are generally similar to those for potassium, particularly in respect of the total potential function $V^T(Q)$ and its Fourier transform in real space. The screened pseudopotential derived assuming the Heine-Abarenkov dielectric constant,[26] is shown in Fig. 8 (curve D), together with that computed by Animalu[22] (curve B). The final oscillation in curve D near Q_{max} is not significant; the experimental data for sodium are barely sufficient to specify the pseudopotential at this range. Indeed, a rather satisfying fit to the data can be obtained with $(a/2\pi)Q_{max}$ as low as 1.3, in confirmation of the earlier work,[5] shown in Fig. 8 as

[27] M. D. Johnson, P. Hutchinson, and N. H. March, Proc. Roy. Soc. (London) **A282**, 283 (1964). See also J. E. Enderby and N. H. March, Advan. Phys. **14**, 453 (1965).

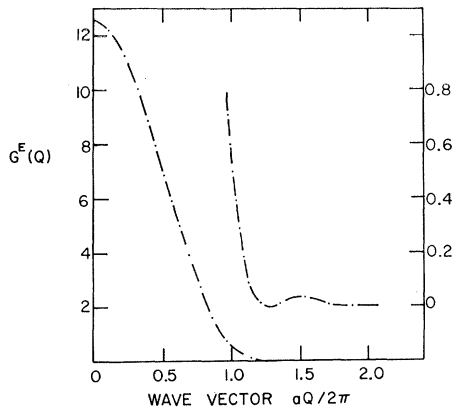

FIG. 9. The function $G^E(Q)$ for sodium derived from curve D of Fig. 8. The large wave-vector region is shown on a 10× scale on the right. The cutoff is at 2.0.

open circles. The function $G^E(Q)$ derived from curve D of Fig. 8 is shown in Fig. 9. Up to a wave vector $(aQ/2\pi)=1.2$, this function is almost indistinguishable from the analogous curve obtained by Cochran. (Beyond this point, Cochran's G function is virtually zero.)

Dispersion curves for potassium have also been calculated by Krebs[28] on the basis of a model in which (a) short-range forces between an atomic and its first and second nearest neighbors are described by only two empirical "force constants," and (b) an arbitrary analytic form is used to describe the screened pseudopotential. The three disposable parameters of the model are fitted to the measured elastic constants, and the calculated normal-mode frequencies are in surprisingly good agreement with our measurements, the average (largest) discrepancy being about 5% (14%). From the foregoing discussion, however, it is clear that there is little physical justification for assuming a contribution (a), particularly in the two-constant form adopted by Krebs. Nor can the use of the "Wigner-Seitz" function in the specification of the screened electron-ion interaction be justified in detail. Its analytic form merely has qualitatively the desired behavior. The Krebs model would nevertheless appear to be a quite convenient alternative to the conventional Born–von Kármán analysis.

4. CONCLUSIONS

The frequencies of the normal modes of vibration of potassium have been measured at 9°K for propagation directions along symmetry lines to an accuracy of about 2%. The results are significantly different from those given by ultrasonic measurements of the elastic constants.[16] Possibly this arises from different modes of propagation of sound at frequencies $<10^9$ cps and $>5\times10^{11}$ cps.

The measurements have been used to find the parameters of a conventional axially symmetric Born–von Kármán model which, with forces extending to fifth nearest neighbors, gives an excellent account of the experimental results. This model has been then used to calculate the frequency distribution and specific heat of potassium. At low temperatures the model gives a small but probably significant discrepancy with the measurements of the specific heat[18]; this may be associated with the elastic-constant behavior.

The experimental results have also been used to deduce pseudopotentials for the electron-phonon interaction, following the work of Cochran.[5,6] These potentials are in quite close agreement with that found by Bortolani[23] using the method of Heine and Abarenkov.[26] The shapes of these potentials are largely independent of their range in reciprocal space, so that we may conclude they are physically quite well defined, and that the measurements lead fairly unambiguously to the pseudopotentials. It is probably worth commenting that the screened pseudopotential changes sign very close to $2k_F$ (Fig. 5), and so the magnitude of the Kohn effect is expected to be very small in both potassium and sodium, as found experimentally. At the smallest reciprocal lattice vectors, (110) and (002), the curve does have nonzero though small values, and so the band structure is not given exactly by the free-electron approximation.

An alternative method of analysis was also employed to find the interatomic potential between neutral pseudo-atoms. This approach gave results which were very dependent on the range chosen for the potential. When transformed to real space, some of these potentials were of comparatively short range, whereas others had a very long-range oscillatory character. Since both types of potential gave excellent accounts of the experimental results, we must conclude that there is considerable arbitrariness in the choice of an interatomic potential. However, it is difficult to understand the physical origin of these long-range oscillations, since the Kohn effect is so small in these materials. Rather similar considerations result from an analysis of the phonon dispersion curves for sodium. Long-range oscillatory potentials have also been found from an analysis of liquid metal structure factor curves.[27,29] It is perhaps of interest to speculate whether there is also a possibility of fitting these curves by a comparatively short-range potential. This arbitrary behavior did not occur in the pseudopotential analysis, which therefore appears to be physically the more sensible approach at present.

ACKNOWLEDGMENTS

We are grateful to Professor R. Bowers and P. A. Penz for supplying us with excellent single-crystal specimens. We have benefited from discussion with Professor W. Cochran. Technical assistance was provided by E. A. Glaser and A. Bell.

[28] K. Krebs, Phys. Rev. **138**, A143 (1965).

[29] A. Paskin and A. Rahman, Phys. Rev. Letters **16**, 30 (1966).